EGU26-18636 · AS5.11 · X5.235

VIENNA · THU 07 MAY · 10:45–12:30 (CEST)

Indoor Aerosol Characterization on a Shoestring

Recent insights from the EDIAQI project

Jan-David Förster[1], Sebastian Düsing[1], Andrea Cuesta-Mosquera[1], Ulf Winkler[1], Goran Gajski[2], Marko Gerić[2], Jens Voigtländer[1], and Mira L. Pöhlker[1]

[1] Leibniz Institute for Tropospheric Research (TROPOS), Atmospheric Microphysics Department, Leipzig, Germany · [2] Institute for Medical Research and Occupational Health (IMI), Division of Toxicology, Zagreb, Croatia

forster@tropos.de

TROPOS Leibniz Institute for Tropospheric Research

EDIAQI

DOI: 10.5194/egusphere-egu26-18636

15 sites — PRIVATE HOUSEHOLDS

90 days — CONTINUOUS FIELD DATA

10 s resolution — REAL-TIME ACQUISITION & CONTROL

11.2 M records — JSON PAYLOADS TRANSMITTED VIA MQTT

99 % data coverage — HIGH RELIABILITY & ROBUSTNESS

>10 parameters — PNSD, PM, T, RH, CO_2, NO_x, VOC, illuminance, ...

MOTIVATION

Science inside, your children in mind

Indoor air poses a significant health risk, particularly for children with their developing respiratory tract. Establishing causal links between indoor air pollutants and health outcomes in asthmatic children is one of the goals of the EDIAQI project (Evidence Driven Indoor Air Quality Improvement)[1], for which aerosol monitoring in homes and bedrooms is essential, since people spend most of their time indoors, 70% at home and 19% in other indoor locations.[2]

Yet no commercial instrument offers PM (Particulate Matter) and PNSD (Particle Number Size Distribution) monitoring combined in a child-friendly, silent, and fully open package. This gap motivated the development of AQBIE (Air Quality Beacon & Immission Evaluator).

INSTRUMENT & DATA INFRASTRUCTURE

Tying aerosol research to IoT

AQBIE is a compact multi sensor platform built around an ESP32. Connected to local WiFi, customized TASMOTA[3] firmware enables real-time data transmission and remote management, including over-the-air updates via MQTT[4]. Its LVGL[5] user interface displays live values and enables activity logging for emission source attribution. In a 90-day campaign in Zagreb, Croatia, 15 devices across 15 households recorded >11 M data points with 99 % coverage. Each AQBIE consists of 14 custom 3D-printable parts.

PM sensor Bosch BMV080
PM_1, $PM_{2.5}$, PM_{10}

Ambient light sensor
ROHM BH1750FVI

Presence Sensor PIR HC-SR602

Optical particle counter
Alphasense OPC-N3
(T, RH, PM & PNSD 350 nm - 10 µm 12/24 bins optional up to 40 µm)

PM sensor Sensirion SEN66
PM_1, $PM_{2.5}$, PM_{10}, T, RH, CO_2, VOC & NO_x Indices

Microcontroller & touch display
M5Stack Core2 series ESP32 + TF-card slot

Reasons for implementing three PM sensors:

- Intercomparison — bulk vs. single-particle counting, in situ
- Aerosol type classification — exploiting differences in spectral sensitivity
- PNSD — size-resolved particle number concentration (not shown here)

FIELD DATA

Indoor & outdoor tightly bound

Indoor emission events, like cooking, can spike $PM_{2.5}$ concentrations two orders of magnitude above background levels. However, since indoor and outdoor pollution are coupled by an infiltration factor (i), outdoor contributions can be accurately reconstructed from indoor data using statistics.

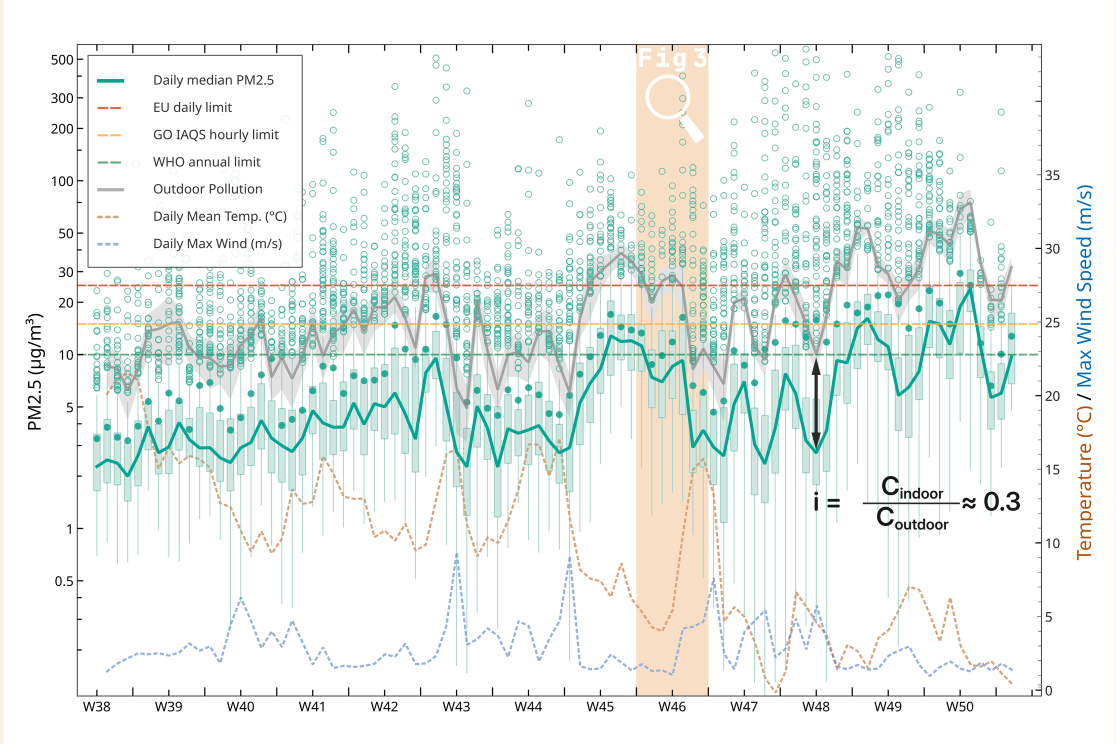

FIG 01 Daily $PM_{2.5}$ concentrations from SEN66 data across 13 AQBIE devices. Outliers in the daily boxes represent indoor emission events; two devices were excluded due to dominant local sources. Daily medians strongly correlate (fig. 2) with outdoor concentrations at four Zagreb reference stations (Zg-1, Zg-2, Zg-4, Mirogojska cesta) and anti-correlate with outdoor temperature and wind speed.

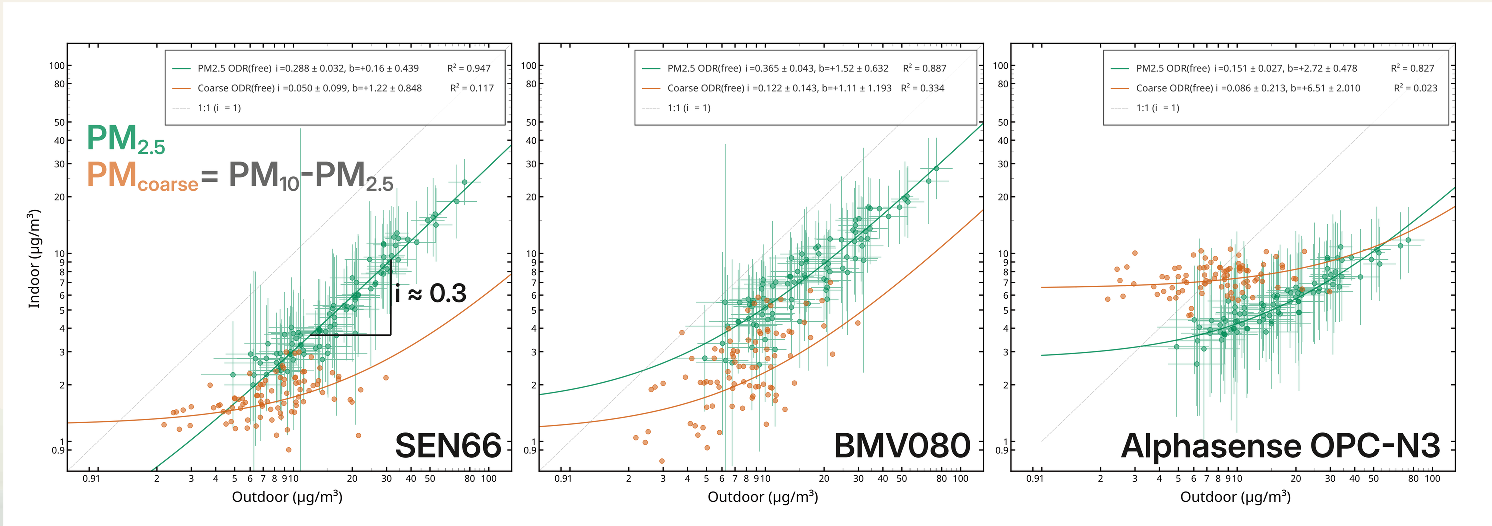

FIG 02 Comparison of the SEN66, BMV080, and OPC-N3 sensor daily median data across 13 devices ($PM_{2.5}$ and PM_{Coarse}) against four equally weighted outdoor reference stations reveals substantial differences in fit quality. The SEN66 achieves the highest correlation for $PM_{2.5}$ ($R^2 = 0.95$), followed by the BMV080 ($R^2 = 0.89$). Infiltration factors decrease for larger particles, consistent with physical expectations.

Correlation strength reflects sensor (spectral) sensitivity to specific aerosol species, not accuracy.

KEY FINDINGS

Atmospheric pattern matching

On an hourly scale, emission peaks must be filtered to isolate the underlying outdoor signal. Air masses at different outdoor reference stations are well-distinguishable and leave their signatures indoors, allowing for the assignment of mixing coefficients to individual devices (tab. 01).

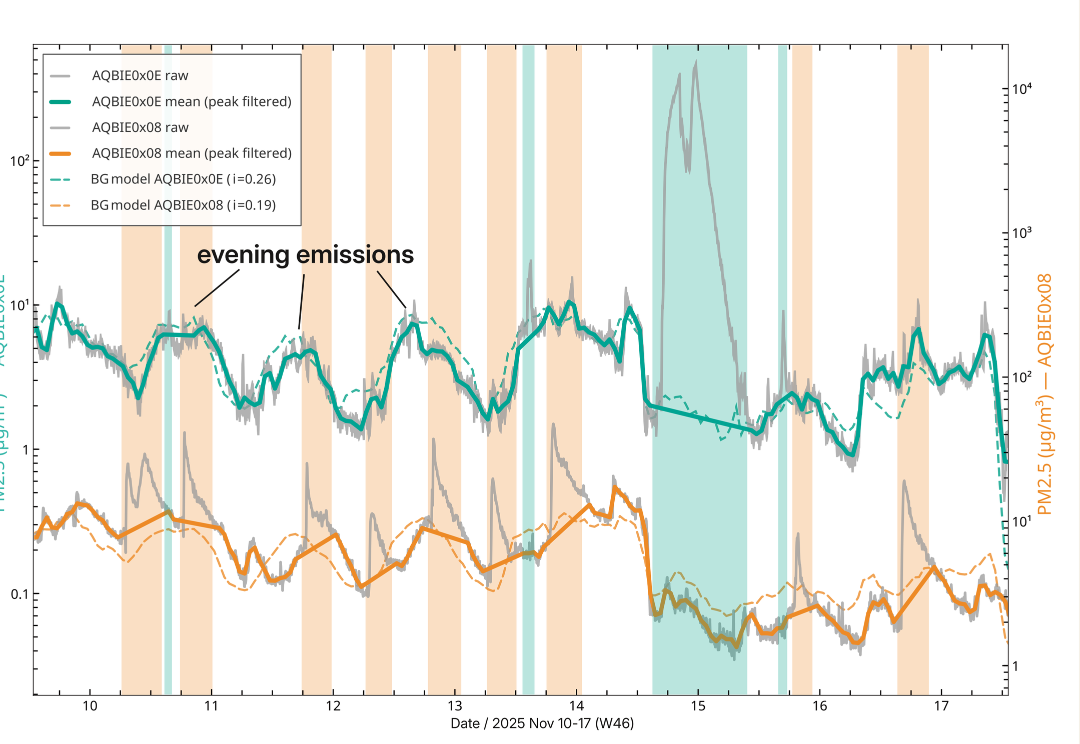

FIG 03 Hourly mean $PM_{2.5}$ time series from SEN66 in W46 (compare fig. 1), filtered for emission peaks, from two AQBIEs, emphasizing the challenge of background determination. For AQBIE0x08, reference-station data between Nov 10 and 14 are phase-shifted due to slowly moving air masses. Dashed lines denote the artificial backgrounds (BG) from mixing reference-station time traces until best match is achieved. (tab. 1)

TAB 01 Result from SEN66 $PM_{2.5}$ reference station mixing and infiltration factor determination for 13 AQBIE sensors, yielding per-station-weights (w_s).

Device ID	R^2	i	w(Zg-1)	w(Zg-2)	w(Zg-3)	w(Zg-4)	w(M.C.)
0x00	0.564	0.18	0.09	–	–	0.10	0.81
0x01	0.739	0.17	0.83	–	0.17	–	–
0x02	0.791	0.41	0.60	–	0.15	0.25	–
0x03	0.706	0.20	0.64	–	0.24	0.12	–
0x04	0.781	0.38	0.25	0.07	0.02	0.46	0.20
0x05	0.453	0.20	–	–	–	–	1
0x06	0.754	0.26	–	–	–	–	1
0x08*	0.605	0.19	–	0.59	0.17	0.05	0.19
0x09	0.691	0.23	0.62	–	–	–	0.38
0x0A	0.414	0.18	–	0.21	0.45	–	0.34
0x0C	0.815	0.34	–	0.26	–	–	0.74
0x0D	0.636	0.30	0.19	0.06	–	–	0.75
0x0E*	0.772	0.26	–	–	–	1	–

Infiltration factors found are in good agreement with Lunderberg et al. (2023).[7] Starred devices in fig. 3.

BEYOND THE MEASUREMENTS

Mapping spatial footprints

The application of an inverse distance weighting (IDW) model[6] (eq. 1) to estimate device coordinates from regression weights yielded mixed results (fig. 4A). As these discrepancies cannot be attributed to wind effects, they likely reflect the influence of local emission sources and urban topology.

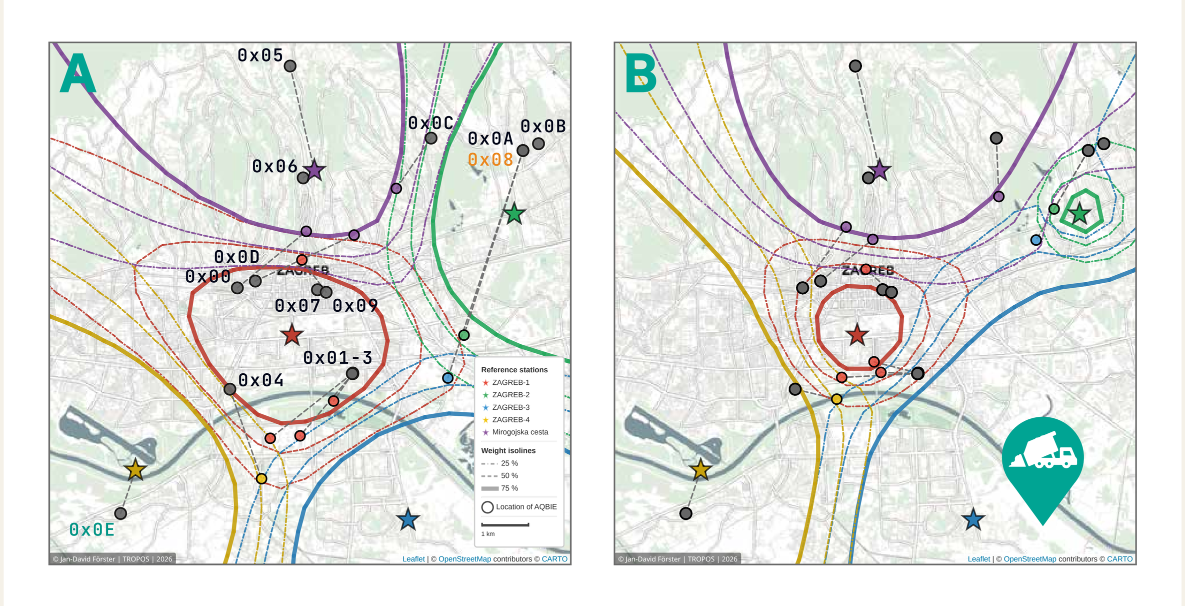

FIG 04 A: Uniform station weighting. Unscaled boundary-stable IDW mixing fractions f_s across the reference station network. B: Optimized station weights after minimizing the total Haversine discrepancies (dashed lines). Scale factors expand/shrink each station's area of influence, for improved device localization. Device coordinates derived from Google Geolocation API using WiFi AP BSSIDs and signal strength. (accuracy < 20 m)

$$w_s(x) = \frac{1}{d_s(x)^r} \exp\left(-\frac{d_s(x) - d_{min}(x)}{B}\right)$$

$x = (\phi, \lambda)$	Candidate point (latitude, longitude)
s	Index of a reference station
$d_s(x)$	Haversine distance from ref. station s
$d_{min}(x)$	Distance to the nearest station
$r = 2$	Distance power (fixed)
$B = 0.3 \times \bar{d}_{inter}$	Bandwidth . $\bar{d}_{inter}$: Mean pairwise distance between all reference stations

EQ 01 Station-wise boundary-stable IDW approach. $B \to 0$: hard Voronoi tesselation; $B \to \infty$: pure IDW

After station-scale optimisation (fig. 4B), the model distinguishes regional from local emission stations and adjusts the influence areas of individual stations. Zg-3's large reach likely links evening & nocturnal PM emissions (fig. 3) to Prudinec-Jakuševec landfill activities.[8,9]

CONCLUSION & OUTLOOK

- Indoor data effectively reconstructs outdoor $PM_{2.5}$ patterns. Distributed AQBIE sensors are valid tools for city-scale air quality monitoring.
- By mapping the found atmospheric footprints, AQBIE complements reference station measurements and provides a basis to question and refine the assignment of reference stations to specific urban areas.
- High-dimensional AQBIE data will be ideal for machine learning-based analysis. Furthermore, sensor spectral sensitivity to specific aerosol species will facilitate advanced source apportionment.

REFERENCES

[1] EDIAQI Project (2025) Air Quality Beacon and Immission Evaluator. *https://ediaqi.eu/articles/air-quality-beacon-and-immission-evaluator-turning-indoor-air-data-action*
[2] Matz, C. J. et al. (2014) Int. J. Environ. Res. Public Health, 11(2), 2108–2124. https://doi.org/10.3390/ijerph110202110
[3] Tasmota (2026) Documentation *https://tasmota.github.io/docs/*
[4] MQTT.org (2026) Protocol Specification. *https://mqtt.org/*
[5] LVGL (2026) Lightweight Graphics Library. *https://lvgl.io/*
[6] Shepard, D. (1968) *Proc. ACM '68*, pp. 517–524. *https://doi.org/10.1145/800186.810616*
[7] Lunderberg, *D. M. et al.* (2023) *PNAS 120 (50) e2308832120, https://doi.org/10.1073/pnas.2308832120.*
[8] Vadić, V. (2006) *Arch. Hyg. Toxicol.*, 57(3), 317–324.
[9] Beli, I., Mihajlović, D. & Vai, V. (2025) *Int. Conf. Air Protection* 2025, p. 24. *https://shorturl.at/eTD1s*

ACKNOWLEDGEMENTS

This work is supported by the affiliated institutions, and funding is provided under the Horizon Europe project EDIAQI (grant ID: 101057497). The authors thank the TROPOS mechanical and electronics workshops for their support and fruitful discussions, as well as Cynthia Odari from EMQ Technologies for providing us with their MQTT broker software EMQX. Furthermore, we would like to thank Theo Arends (https://github.com/arendst), Stephan Hadinger (https://github.com/s-hadinger), and the community around the open-source project Tasmota for their contributions and ongoing development.

Leibniz Association